Medical Image Segmentation by Water Flow

Xin U Liu, Mark S Nixon

ISIS Group, School of ECS, University of Southampton, UK

Abstract. We present a new image segmentation technique based on the paradigm of water flow and apply it to medical images. The force field analogy is used to implement the major water flow attributes like water pressure, surface tension and adhesion so that the model achieves topological adaptability and geometrical flexibility. A new snake-like force functional combining edge- and region-based forces is introduced to produce capability for both range and accuracy. The method has been assessed qualitatively and quantitatively, and shows decent detection performance as well as ability to handle noise.

1. Introduction

Segmenting anatomical structures from medical images is a fundamental step in analysing medical data. For example, the retina vessel structures can provide useful information like vessel width, tortuosity and abnormal branching which are helpful in diagnoses. Manual delineation of the structures is ineffective and inefficient especially when the number of images is large. Therefore, automatic analysis is needed. However, the complexity and variability of the anatomical features, together with the imperfections of typical medical images such as intensity inhomogeneities and imaging noise which cause the boundaries of structures of interest discontinuous or indistinct, make the automatic segmentation very challenging.

Many methods have been proposed in medical image segmentation. Active contours or snakes [1] are one of the powerful segmentation techniques. An active contour is essentially a parameterized curve which evolves from an initial position to the object's boundary following some rules so that a specified energy functional can be minimized. The methods achieve many desirable features including inherent connectivity and smoothness that counteract object boundary irregularities and image noise. Therefore, they provide an attractive solution to the medical image segmentation problem. However, there are still many limitations. Classical parametric snakes use edge information and need good initialization for a correct convergence. Moreover, they cannot handle topological and geometrical changes like object splitting or merging and boundary concavities. Many methods have been proposed to overcome these problems. The balloon models [2], distance potentials [3], and gradient vector flow (GVF) [4] have been developed to solve the problems of initialization and concave boundary detection. Snake energy functionals using region statistics or likelihood information have also been proposed [5, 6]. A common premise is to increase the capture range of the external forces to guide the curve towards the boundaries. For complex topology detection, several authors have proposed adaptive methods like the T-snake [7] based on repeated sampling of the evolving contour on an affine grid. Geometric active contours [8, 9] have also been developed where the planar curve is represented as a level set of an appropriate 2-D surface. They work on a fixed grid and can automatically handle topological and geometrical changes. However, many methods solve only one problem whilst introducing new difficulties. Balloon models introduce an inflation force so that it can "pull" or "push" the curve to the target boundary, but the force cannot be too strong otherwise "weak" edges would be overwhelmed. Region-based energy can give a large basin of attraction and can converge even when explicit edges do not exist but it cannot yield as good localization of the contour near the boundaries as can edge-based methods. Level set methods can detect complex shapes well but also increase the complexity since a surface is evolved rather than a curve.

Many region merging and growing techniques rely on the assumption that adjacent pixels in the same region have similar characteristics such as intensity, texture or colour. They test the statistics inside different adjacent regions and then decide whether or not they can be merged according to the specified homogeneity criterion. The methods are free of topological changes since they are pixel-wise techniques without smoothness constraints [10]. However, this feature tends to yield irregular boundaries and small holes, especially for noisy images [11]. Besides, the region statistics comparison standards on which they are based can lead to inaccurate contour detection.

Another shortcoming of active contours and region merging methods, both of which are mathematical models, is the difficulty of explaining the abstract operation principles, model variables and parameters. In comparison, physical models have the fundamental advantage that the working principles, input and output are all explicit and material and hence are easy to interpret and debug. The physical model we propose is based on water flow analogy because the features of water like fluidity and surface tension can lead to topological adaptability and geometrical flexibility, as well as contour connectivity and smoothness. In this paper, the force field analogy [12], which is highly robust to noise, is adopted to define the resultant force of water pressure, surface tension and adhesion, instead of the binary convolution method and the gradient of 'clipped' edges [13, 14]. This provides a more solid and complete theoretical

basis for the framework. The method shows encouraging performance on synthetic and real images. A quantitative performance evaluation is also presented to show noise robustness of the new operator, compared with the level set method based on region statistics [6].

2. Water flow model

The new technique aims to detect objects with closed shapes (simple or complicated) accurately whilst retaining a smooth shape. We thus use the analogy to water flow, which is a compromise between several factors: the position of the leading front of a water flow depends on pressure, surface tension, adhesion/capillarity. There are some other natural properties like turbulence and viscosity, which are ignored here. Image edges and some other characteristics that can be used to distinguish objects are treated as the "walls" terminating the flow. The final static shape of the water will describe the related object's contour.

The flow is determined by pressure and the resistance. The relationship between the flow rate f_r, the flow resistance R and the pressure difference, is given by:

$$f_r = (P_i - P_o)/R \tag{1}$$

where P_i and P_o are pressure of the inflow and outflow, respectively. The pressure difference drives the flow and

$$f_r = AV_{effective} \tag{2}$$

where A is the cross-sectional area and $V_{effective}$ is the effective flow velocity. Hence the velocity can be related to force and resistance through equations (1) and (2).

There are small discontinuities or weak regions existent on the contours which may lead to "leakage" of water. The surface tension, which can form a water "film" to bridge gaps, is then applied to overcome the problem. There is an attractive force, named adhesion, existing between water and walls. It is also adopted in the new technique so as to assist surface tension to bridge edge gaps and allow flow into narrow braches.

2.1 Framework of the water flow analogy

One pixel in the image is considered to be one basic unit of the water. The water pressure is defined as the resultant force of the repulsive forces between the water elements. The elements on the water contour, however, are considered to attract other contour elements, and hence generate surface tension. The image edges that are not flooded produce attractive forces and the total attraction is defined as the adhesion.

The flow process is assumed to be made up of two separable steps. The first stage is *acceleration*: the contour element achieves a velocity due to the presence of the water pressure, surface tension and any adhesive force, and the ultimate value is given by equations (1) and (2). The next step is *exterior movement* where the moving element is now free from the influence of other water elements and suffers only external image forces. This is not consistent with real action but is sufficient for the digital image analogy and greatly simplifies the algorithm.

The water element can move outwards in any direction for which the component of velocity is positive. However, only if the velocity is sufficiently large, can the element break through the image resistant forces and 'flood' an adjacent 'dry' position. To reconcile the flow velocity with forces, dynamical formulae are used. Here, the definitions of kinetic energy and resistant work are used. Given an element with mass m, a positive velocity v on a particular direction and is acted by the force F during the process, if the element can arrive at the direction-related position after a displacement S, then this inequality must be fulfilled:

$$FS + mv^2/2 \geq 0 \tag{3}$$

where force F is scalar that is positive when it is consistent with velocity v, and negative otherwise. The inequality means that only if the initial kinetic energy given by water forces could exceed the resistant work given by the image force, can the element finally flow to the target position.

2.2. Force field, water forces, and flow velocity

In this new water flow model, each water element is treated as a particle exhibiting attraction or repulsion to other ones, depending on whether or not it is on the surface. The adhesive force, essentially, is determined by the attractive forces from the adjacent edge points. These facts demonstrate a link between the new model and the force field analogy [12]. Both water elements and the image pixels that are not flooded are treated as arrays of mutually

attracted or repelled particles acting as the source of a Gaussian force field. *Gauss's law* is used as a generalization of the inverse square law which defines the gravitational and electrostatic force fields. Denoting the mass value of pixel with position vector $\mathbf{r}_i$ as $L(\mathbf{r}_i)$, we can define the total attractive force at $\mathbf{r}_i$ from other points within the area $\mathbf{W}$ as

$$\mathbf{F}(\mathbf{r}_i) = \sum_{j \in \mathbf{W}, j \neq i} L(\mathbf{r}_j) (\mathbf{r}_j - \mathbf{r}_i) \Big/ |\mathbf{r}_j - \mathbf{r}_i|^3 \tag{4}$$

The equation can be directly adopted in the water flow model, provided the mass values are properly defined. The magnitude of a water element is set to 1, and that of an image point equals to the corresponding edge strength. The water contour points and the image pixels should be set positive, and the interior water elements should be negative because equation (4) is for attractive forces.

From equations (1) and (2), the flow velocity is inversely proportional to the resistance of water. In a physical model, the resistance is decided by the viscosity, the flow channel and temperature etc. Since this is a physical analogy which offers great freedom in selection of parameter definitions, we can relate the resistance definition to certain image attributes. For instance, in retina vessel detection, if the vessels have relatively low intensity, we can define the resistance to be proportional to the intensity of the pixel. If we derive the resistance from the edge information, the process will become adaptive. That is, when the edge response is strong, resistance should be large and the flow velocity should be weakened. Thereby, even if the driving force set by users is too "strong", the resistance will lower its influence at edge positions and the problem in balloon models [1], where strong driving forces may overwhelm "weak" edges, can be suppressed. We first write an equation of velocity by (1) and (2):

$$\mathbf{V}(\mathbf{r}_i) = \mathbf{F}(\mathbf{r}_i) / A \cdot R \tag{5}$$

where $\mathbf{V}(\mathbf{r}_i)$is the resulting flow velocity. In this paper, A is set as a constant, and R at position (u, v) is determined by

$$R = \exp\{k \cdot \mathbf{E}(u,v)\} \tag{6}$$

where $\mathbf{E}$ is the edge strength matrix and k controls the fall of the exponential curve. If we assign a higher value to k, the resistance would be more sensitive to the edge strength, and a lower k will lead to less sensitivity.

2.3. Image force

During the *exterior movement* step, the moving element is acted solely by the image force, which is a combination of edge-based and region-based force functionals. The edge potential force is defined as the gradient of an edge response map since it gives rise to vectors pointing to the edge lines [4]. The force is large only in the immediate vicinity of edges and always pointing towards them. The potential force on a contour element (x_c, y_c) is given by:

$$\mathbf{F}_P = \nabla \mathbf{E}(x_t, y_t) \tag{7}$$

where $\nabla \mathbf{E}$ is the gradient of the edge map, and (x_t, y_t) are the coordinates of the flow target because the potential force is presumed to act during the second stage of flow where the element has left the contour and is moving to the target.

The forces defined above work well as long as the gradient of edges pointing to the boundary is correct and meaningful. However, as with corners, the gradient can sometimes provide useless or even incorrect information. Unlike the method used in the inflation force [2] and T-snake [7], where the evolution is turned off when the intensity is bigger than some threshold, we propose a *pixel-wise* regional statistics based image force. The statistics of the region inside and outside the contour are considered respectively and thus yield a new image force:

$$F_S = -\frac{n_{int}}{n_{int}+1}(\mathbf{I}(x_t, y_t) - \mu_{int})^2 + \frac{n_{ext}}{n_{ext}-1}(\mathbf{I}(x_t, y_t) - \mu_{ext})^2 \tag{8}$$

where subscripts "*int*" and "*ext*" denote inner and outer parts of the water, respectively; μ and n are the mean intensity and number of pixels of each area, separately; $\mathbf{I}$ is the original image. The equation is deduced from the Mumford-Shah functional used by Chan's level set operator [6] and the derivation has been shown in [13, 14].

Edge-based forces provide a good localization of the contour near the real boundaries but have limited capture range whilst region-based forces have a large basin of attraction and relatively low detection accuracy. A convex combination method is chosen to unify the two functionals:

$$F = \alpha F_P + (1 - \alpha) F_S \tag{9}$$

where all terms are scalar quantities where a positive value means the direction is from the origin to the target flow position, and α ($0 \leq \alpha \leq 1$) is chosen by the user to control the balance between them.

Movement decision process

If the *acceleration stage* gives an initial velocity pointing outwards, inequality (3) will be used to determine whether or not the element could reach the target position in the second flow stage. Each possible target position will be tested separately. As all the terms in inequality (3) are scalars, the velocity given by equation (5) will be decomposed. The scalar terms will be positive if they point from the origin to the target. In inequality (3) and equation (5), there are parameters like m, S and A which are defined as constant. For simplicity, we divide the two sides of inequality (3) by S, combine all the constant parameters and hence get the movement decision processor:

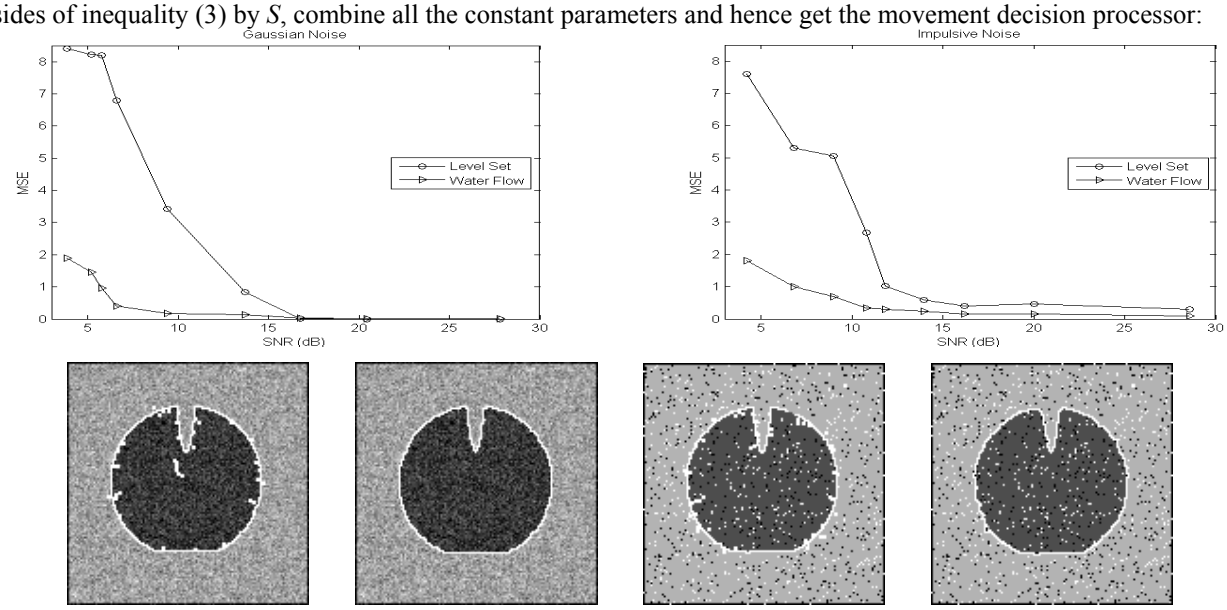

(a) LS (MSE: 0.83) (b) WF (MSE: 0.13) (c) LS (MSE: 1.02) (d) WF (MSE: 0.31)

Figure 1. Quantitative evaluation and detection examples for level set method (LS) and water flow operator (WF).

$$\lambda v^2 + F \geq 0 \tag{10}$$

where λ, the combination of mass m, displacement S and area A, is a regularization parameter set by users controlling the trade-off between the two energy terms. In total, if the initial flow velocity v is positive, and inequality (10) can be satisfied, the water element will move to the corresponding direction and flood the target position.

3. Experimental Results

3.1. Quantitative evaluation

A quantitative result assessment is performed as shown in figure 1. The level set method based on region statistics [6] is chosen for comparison. The test image is synthetic in order that the ideal result can be achieved. The object of interest is designed with a boundary concave to increase the detection difficulty. Different levels of Gaussian and Impulsive noise are added. The mean square error (MSE) is used to measure the performance under noise.

$$MSE = \sum_{k=1}^{I_D} d_k^{\,2} \Big/ \max(I_D, I_I) \tag{11}$$

where I_I and I_D are the number of ideal and detected contour points respectively and d_k is the distance between the kth detected contour point and the nearest ideal point. For both noise, the performance of the water flow model is markedly better than the level set operator especially when the noise contamination is severe (SNR less than 10dB). The performance superiority of the new operator under noisy conditions is further illustrated qualitatively by the segmentation results for Gaussian noise (SNR: 13.69) and impulsive noise (SNR: 11.81), see figure 1 (a) to (d). This robustness to noise is desirable for medical image segmentation as discussed in Section 1.

3.2. Natural medical images

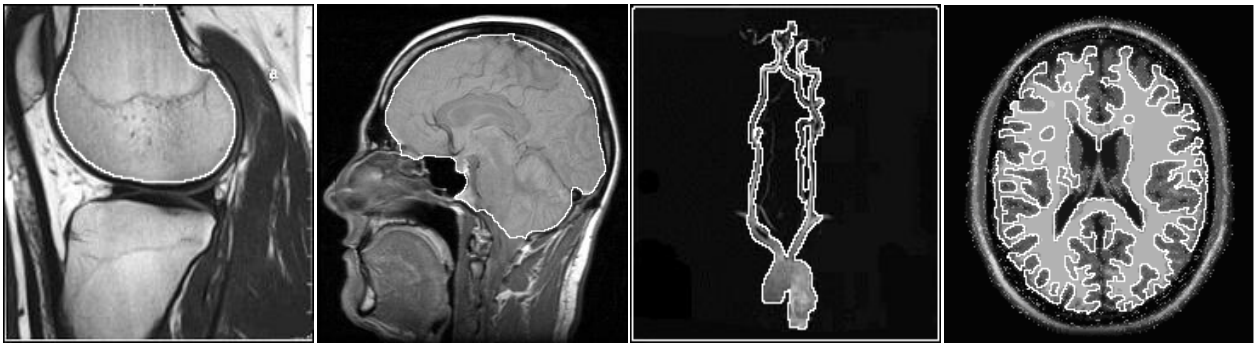

(a) (b) (c) (d)

Figure 2. Segmentation results in real medical images: a) femur in MR knee image, b) brain in a sagittal MR image, c) carotid artery in a MR carotid MRA image and, d) grey/white matter interface in MR brain image slice.

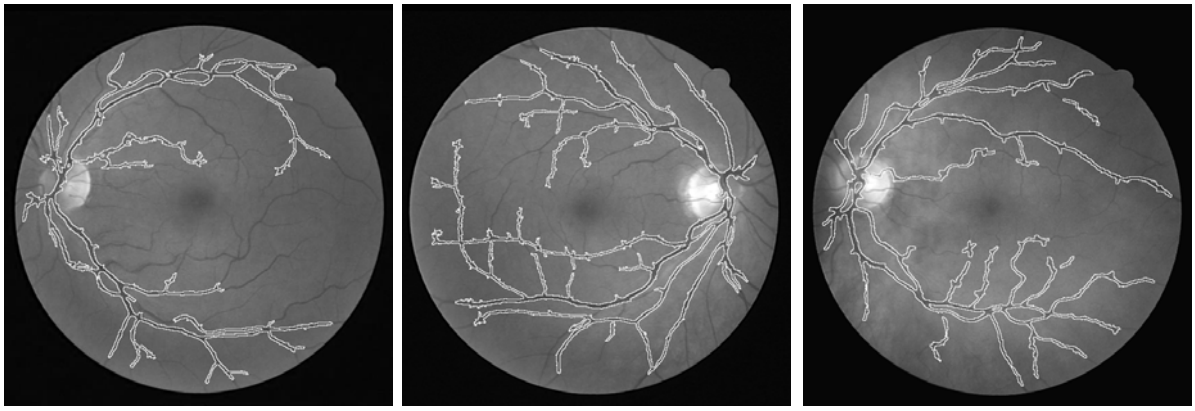

(a) (b) (c)

Figure 3. Segmenting vessels in retinal images with low resolution and quality (k=50, α=0.5, λ=1)

We applied the new model to natural medical images. Figure 2 presents the segmentation results for MR images. The water sources are all set inside the object of interest and parameter are chosen as k=50, α=0.5, λ=1. The resultant contours are relatively smooth by virtue of surface tension. The operator can find weak-contrasted boundaries as shown by figure 2 (b) where the indistinct interface between the brain and the spine is detected. This is achieved by combining a high value of k that gives the operator a high sensitivity to edge response and the region-based forces. The fluidity of water leading to topological adaptability and geometrical flexibility is fully realised. Figure 2 (c) and (d) illustrate this – the complex structures and irregular branches are segmented successfully.

Retinal vessel segmentation plays a vital role in medical imaging since it is needed in many diagnoses like diabetic retinopathy and hypertension. The irregular and complex shape of vessels requires the vessel detector to be free of topology and geometry. Furthermore, digital eye fundus image often have problems like low resolution, bad quality and imaging noise. The water flow model is a natural choice. Figure 3 shows the segmentation results. In figure 3 (a), only one water source inside the vessels within the optic disk is initialised. We can see that the major vessel structure has been detected, and the result is a single, connected structure. By setting multiple initialisations, more complete results can be achieved as shown in figure 3 (b) and (c). In figure 3 (b), multiple flows of water merged, leading to a single vessel structure. In 3 (c), some flows merged and some remained separated. This can be improved by post-processes like gap-linking techniques.

4. Conclusion

This paper combines the water flow model with force field analogy. This provides the physical framework a more theoretically sound and complete basis. The desirable features of water such as fluidity and surface tension are gained, leading to topological adaptability, geometrical flexibility, and segmentation smoothness. The immunity to noise which is enhanced by embodying force field paradigm also helps to make it suitable for medical image processing. The application of the model to MR and eye fundus images illustrates great potential of the method. Note that this is a general framework and can be combined with more refined edge/region detectors to achieve better performance, and the physical feature of the model makes it straightforward to be extended to the segmentation of 3D volumes.

References

[1] M. Kass, A. Witkin and D. Terzopoulos, "Snakes: Active contour models," *Int'l. J. of Comp. Vision,* 1(4):321-331, 1988

[2] L. D. Cohen, "On active contour models and balloons," *CVGIP, Image Understanding,* 53(2): 211-218, 1991.

[3] L. D. Cohen and I. Cohen, "Finite element methods for active models and balloons for 2-D and 3-D images," *IEEE Trans. PAMI,* 15: 1131-1147, 1993.

[4] C. Xu and J. L. Prince, "Snakes, shapes, and gradient vector flow," *IEEE Trans. Image Processing,* 7(3): 359-369, 1998.

[5] M. Figueiredo and J. Leitao, "Bayesian estimation of ventricular contours in angiographic images," *IEEE Trans. Medical Imaging,* 11: 416-429, 1992.

[6] T. F. Chan and L. A. Vese, "Active contours without edges," *IEEE Trans. Image Processing,* 10: 266-276, 2001.

[7] T. McInerney and D. Terzopoulos, "Topologically adaptive snakes," *Int'l Conf. Computer Vision,* pp. 840-845, 1995.

[8] V. Casselles, R. Kimmel, and G. Spiro, "Geodesic active contours," *Int'l Journal of Computer Vision,* 22(1):61-79, 1997.

[9] R. Malladi et al., "Shape modeling with front propagation: A level set approach," *IEEE Trans. PAMI,* 17: 158-174, 1995.

[10] R. Adams, and L. Bischof, "Seeded region growing," *IEEE Trans. PAMI,* 16(6): 641-647, 1994.

[11] S.C.Zhu and A.Yuille, "Region competition: unifying snakes, region growing, and Bayes/MDL for multi-band image segmentation," *IEEE Trans. PAMI*, 18(9): 884-900, 1996.

[12] D. J. Hurley, M. S. Nixon, and J. N. Carter, "Force field feature extraction for ear biometrics," *CVIU,* (98): 491-512, 2005.

[13] X. U. Liu and M. S. Nixon, "Water flow based complex feature extraction," *Acivs 2006*, pp. 833-845, 2006.

[14] X. U. Liu and M. S. Nixon, "Water flow based vessel detection in retinal images," VIE 2006, pp. 345-350, 2006.